Influence of microstructure and heat treatment on corrosion in new low-lead and lead-free brass alloys

Emil Stålnacke; Erik Claesson; Charlotta Obitz; Mirjam Lilja; Joacim Hagström and Olivier Rod*

* Swerea KIMAB AB, Box 7047, SE-164 07 Kista, Sweden , Tel: +46 8 440 48 39, olivier.rod@swerea.se,

Abstract

In new low-lead and lead-free brass alloys, it is not understood how the corrosion properties, such as dezincification, are related to material composition as well as annealing temperature and duration. This study aims to fill this knowledge gap by mapping sixteen annealing conditions within the temperature range 250°C – 400°C and three different brass alloy compositions to their respective microstructure and dezincification performance. The three investigated alloys were CW511, CW625 and CW626. It was found that high dezincification depth was a result of precipitation of intermetallic AlAs-particles along grain boundaries, twins and lead particles as well as precipitation of β-phase along grain boundaries. The precipitations of these phases were promoted by annealing temperatures within 300°C – 400°C, especially for extended annealing durations. The alloys with high micro additions of aluminium or iron were the most susceptible to this dezincification attack. In addition, it was discovered that the alloy with high aluminium content and low copper/zinc-ratio exhibited higher amount of β-phase, thus emphasizing the role of the copper/zinc-ratio in the corrosion resistance of brass alloys.

Introduction

Brass is a copper alloy containing zinc as its main alloying element [1]. An important application of many commercial brass alloys involves transport of drinking water, including plumbing and fittings. In this environment, brass can be subject to a corrosion mechanism called dezincification, in which zinc is selectively removed from the brass, thus leaving a porous copper matrix with poor mechanical properties that can result in crack propagation and mechanical failure [2]. To prevent this, various manufacturers add micro-additions (0.03%) arsenic to their alloy. [1, 3–7]

Arsenic dissolves in solid solution within the dominant phase of these alloys, the face centred cubic α-phase [2, 6, 7] which significantly increases its dezincification resistance [1].

However, poor heat treatment can reduce this beneficial effect by precipitating the zinc-rich body centred cubic β-phase. Arsenic cannot protect the β-phase from dezincification so the alloy is thus vulnerable to dezincification attacks [1].

Furthermore, investigations have reported that heat treatment at certain annealing temperatures, generally in the range 300°C – 400°C [6], results in the arsenic forming intermetallic arsenide particles with other elements in the alloy, including aluminium and iron [1,8], which are added to enhance castability and grain refining [1, 3, 9]. The formation of arsenide particles depletes the active arsenic content, so deteriorating the dezincification protection of the α-phase and sensitizing it to dezincification attack [9, 10]. This transformation is a diffusion controlled process [1] and it is often observed that intermetallic arsenide particles precipitate adjacent to grain boundaries due to the higher lattice disorder there compared to the grain interiors. Thus, grain boundaries are subject to dezincification attack, also referred to as grain boundary attack or intergranular attack (IGA) [7, 9, [11]. With careful heat treatment, precipitation of both β-phase and arsenide particles can be avoided [1]. Brasses with arsenic successfully protecting the material from dezincification are appropriately referred to as dezincification resistant brass alloys (DZR) [11].

Lead has traditionally been added to brass in contents of a few percent to improve its hot workability and machinability in many types of water fittings. However, it has been found that lead leaches into the drinking water at too high concentrations, thus promoting several countries and institutes, including the 4 Member State Joint Committee, to propose more strict regulations regarding the maximum allowed amount of lead in the material composition [12]. Since lead has been a crucial element for enhanced machinability [1], a paradigm shift is now taking place within the brass manufacturing industry in terms of compositional and material design to adjust to the new regulations.

Among some of the new commercially available low lead and lead free brass alloys, aluminium content has been increased and the copper/zinc-ratio has changed. How this affects the microstructure and the dezincification properties is not well understood. One reported issue with the new alloys is that their corrosion protection is depleted during stress relieving heat treatment, which is performed after all cold deformation treatments, including machining [13]. For manufacturers of water fittings and plumbings, minimizing residual stresses is crucial for avoiding stress corrosion cracking [1, 6], thus this is problematic since manufacturing these products requires cold deformation and machining.

To enable the industry to make more informed decisions in choosing annealing conditions for the new low lead and lead free brass alloys, the present study aims to better understand the influence of stress relieving heat treatment on the dezincification resistance as well as the microstructure of new brass alloys. To accomplish this, three different new low lead and lead free brass alloys have been heat treated using different annealing conditions, and their

resulting microstructures are mapped in relation to their dezincification performance. The experimental results are also related to thermodynamic simulations.

Material

The samples used in this study were obtained from three extruded bars produced by *Nordic Brass Gusum AB*. Each bar represented a different alloy, referred to as CW511L, CW625N and CW626N respectively. Their chemical compositions are given in
Table *1*.

CW511L is commercially considered to be lead free since it contains less than 0.3% lead. The only active elemental addition beyond copper, zinc and lead is arsenic. The remaining elements are considered as impurities which arise from recycled scrap. In addition, the chemical analysis of the CW511L revealed the lowest Cu/Zn-ratio of the three alloys: ~1.78.

CW625N and CW626N are considered as low lead alloys since they contain 1.2 – 1.3% lead. In addition, they have been actively alloyed with additional aluminium and contained slightly higher iron concentrations as compared to the CW511L alloy. The main differences between CW625N and CW626N were the higher Cu/Zn-ratio in the latter, as illustrated in
Table *1*.

Table 1: Chemical composition in weight percent

Alloy	Cu	Zn	Pb	Al	Fe	As	Rem.	Cu/Zn-ratio
CW511L	63.8%	35.9%	0.20%	< 0.05%	0.05%	< 0.10%	< 0.21%	1.78
CW625N	63.7%	34.8%	1.30%	0.60%	0.11%	< 0.10%	< 0.24%	1.83
CW626N	64.6%	33.2%	1.23%	0.70%	0.11%	< 0.10%	< 0.20%	1.95

Method

Samples cut from the extruded bars were heat treated in muffle furnaces in two steps. First they were pre-heated at 550°C for 2h in order to minimize the volume fraction of β-phase and to ensure a common thermodynamic starting point. Thereafter the samples were annealed at either 250°C, 300°C, 350°C or 400°C for 2 hours, 10 hours, 100 hours or 1000 hours. The temperatures in both heat treatment steps were monitored using two thermocouples; one measured the ambient temperature and the other the temperature of the largest sample in the furnace. After each heat treatment, the samples were cooled in air to 25°C. Samples without any heat treatment or pre-heating were kept as references

Test samples were cut out into 10mm x 10mm x 10mm cubes from each heat treatment, and mounted in phenolic resin so that the exposed surface was perpendicular to the extrusion direction of the original bar. The exposed surface was ground to 600 mesh size using wet abrasive SiO_2-paper. Dezincification testing was performed in accordance with the Swedish standard ISO 6509 "Corrosion of metals and alloys – Determination of dezincification resistance of copper alloys with zinc" of the *Swedish Standard Institute* (SSI) [14]. According to this, the samples were exposed to 1% $CuCl_2$ solution for 24h ± 30min at 75°C.

After exposure, the exposed surface was sectioned parallel to the extrusion direction in order to examine the depth of the corrosion. The cross-section was ground down to fine 4000 mesh size using wet abrasive SiO_2–paper, followed by mechanical polishing using cloths with 3μm, 1μm and 0.25μm in diamond suspension successively. The depth of the dezincification attack (average depth and maximum depth) was examined in the optical microscope in accordance with ISO 6509 [14].

The volume fraction of β-phase precipitated in the samples was also measured on the plane parallel to the extrusion direction in the optical microscope. The examined surface had been etched in Klemm's solution for 15 seconds, giving the β-phase a distinct yellow colour. The area fraction of yellow pixels could thus be calculated using the software ImageJ on three representative pictures of the microstructure. Only the samples heat treated for 1000 hours and the samples with no heat treatment were investigated.

The presence of intermetallic arsenide particles in samples was investigated using scanning electron microscopy with EDS and EBSD detectors. Only a few selected samples were investigated. Using the post processing software *Tango* by *Oxford Instruments*, the EBSD results were overlapped with the EDS results. This made it possible to investigate where sites for nucleation of arsenide particles were located in the microstructure.

Thermodynamic calculations were performed in Thermo-Calc, utilising a database for brass developed by Swerea KIMAB. The calculated property diagram would display the simulated mole fraction of each stable phase at each heat treatment temperature, under the assumption that the system has reached equilibrium. This was done in order to assist the analysis of the microstructures.

Results and discussion

Influence of annealing on dezincification resistance

The corrosion resistance was mapped in terms of annealing temperature and duration for the three alloys in order to relate the resulting microstructural precipitates to dezincification resistance. As represented in Figure 1, CW511L maintained high dezincification resistance for all the investigated annealing conditions. Analysis of this microstructure in optical and scanning electron microscopes revealed that neither β-phase nor arsenide particles had precipitated in the annealed CW511L-samples. This means that the dezincification inhibitor arsenic remained in solid solution within the α-phase thus protecting it. Furthermore, the dezincification susceptible β-phase never precipitated from any heat treatment. Thus, it may be expected that CW511L should display a high dezincification resistance.
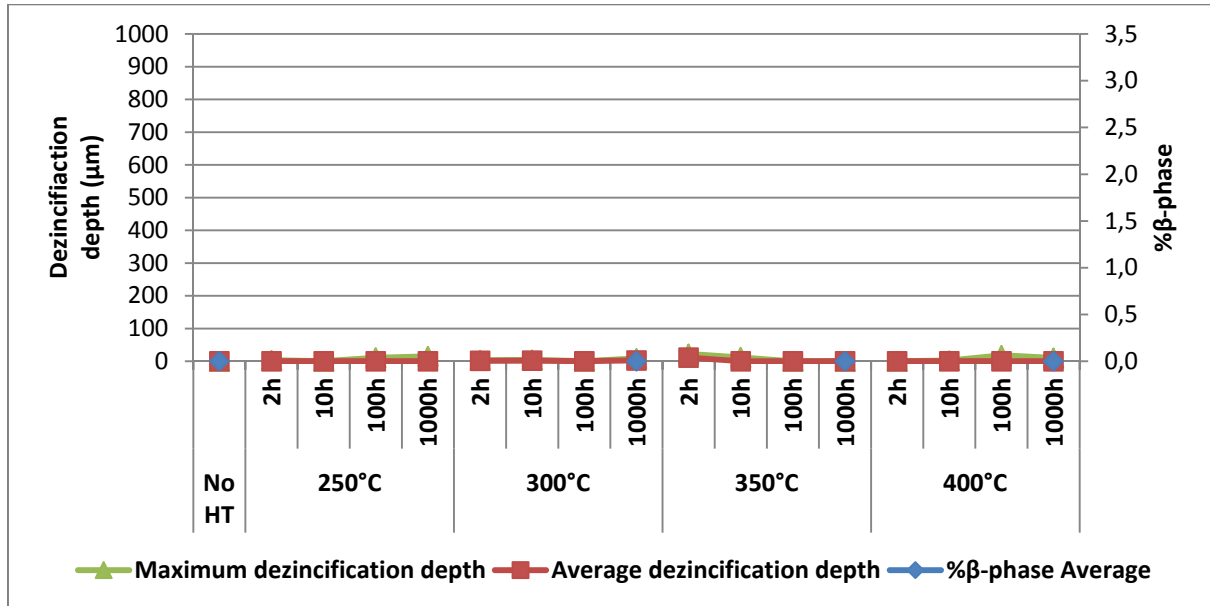

Figure 1: Average and maximum depth of dezincification attack as well as relative area fraction of precipitated β-phase in annealed brass alloy CW511L after accelerated dezincification test in cupric chloride solution.

When comparing CW625N and CW626N in Figure 2 and 3, it is noted that high corrosion resistance was maintained for all annealing conditions at 250°C, as well as the shortest duration (2 hours) at 300°C, 350°C and 400°C. However, both these alloys displayed clear loss of corrosion resistance when annealed for an extended duration at 300°C – 400°C.
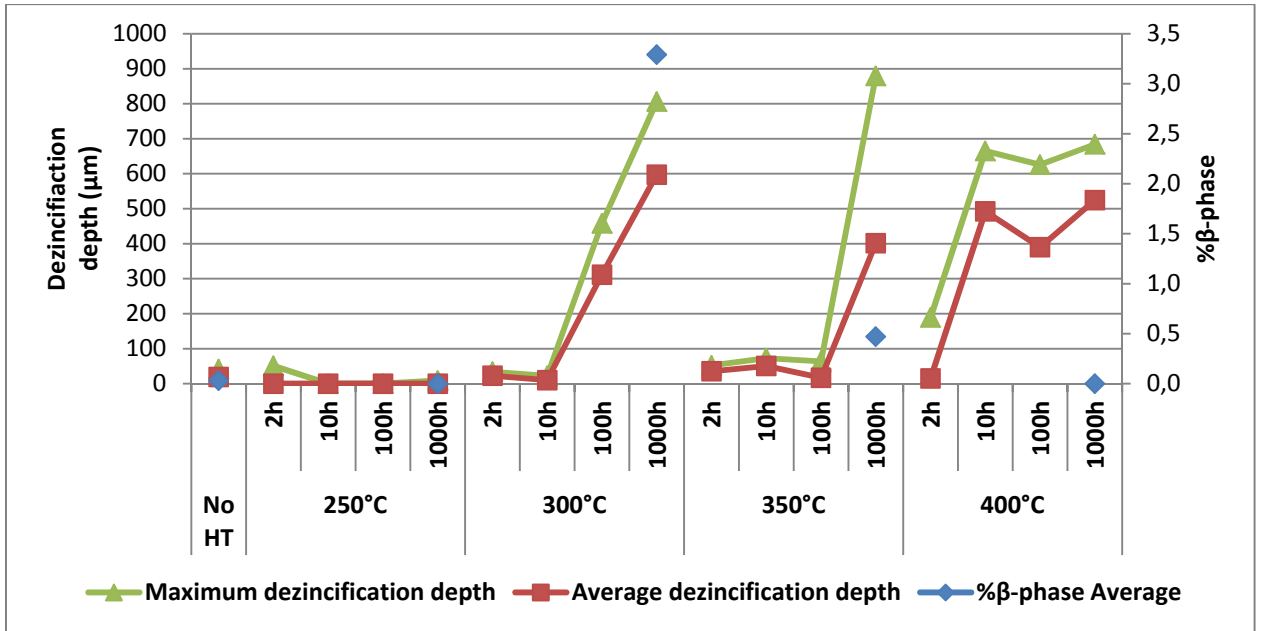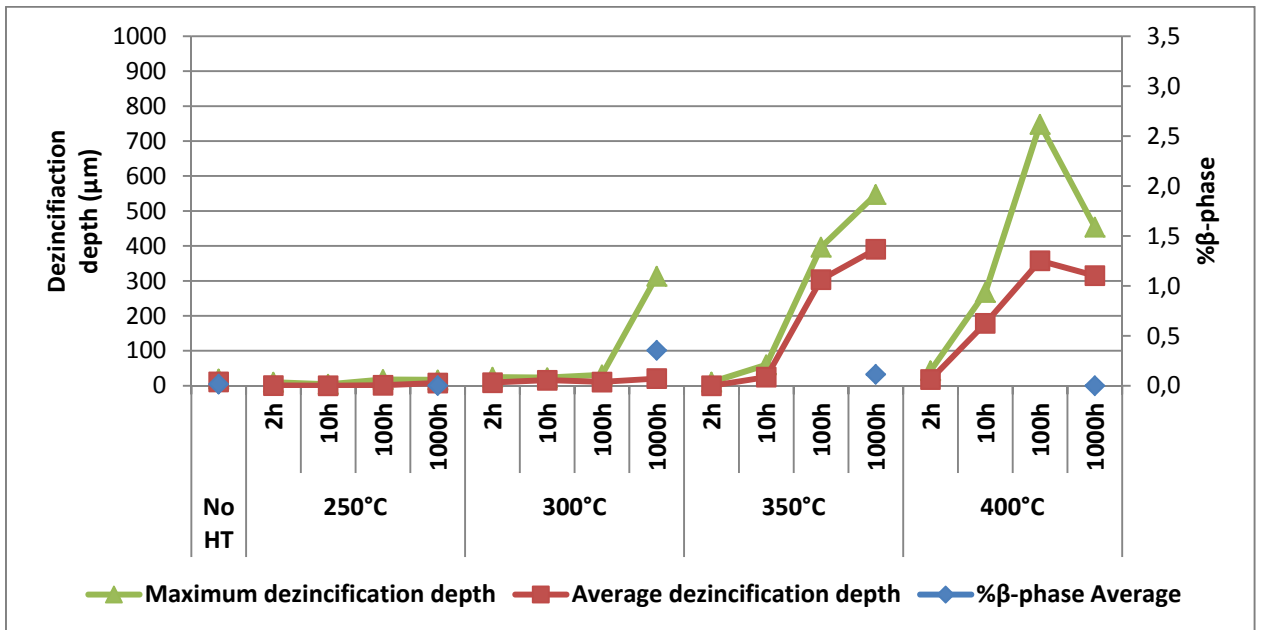
Figure 2: Average and maximum depth of dezincification attack as well as relative area fraction of precipitated β-phase in annealed brass alloy CW625N after accelerated dezincification test in cupric chloride solution.

Figure 3: Average and maximum depth of dezincification attack as well as relative area fraction of precipitated β-phase in annealed brass alloy CW626N after accelerated dezincification test in cupric chloride solution.

Influence of annealing on microstructure

Of the three alloys, CW511L showed negligible dezincification depth for all investigated samples exposed to $CuCl_2$ solution, as represented in Figure 1. As observed in the chemical analysis in

Table *1*, the main difference in composition in CW511L compared to CW625N and CW626N is its significantly lower aluminium and iron contents. Since the heat treatment as well as the corrosion testing and sample preparation of CW511L samples was identical to CW625N and CW626N, which displayed considerably lower dezincification resistance, it is probable that the difference in dezincification resistance is related to the higher aluminium or iron contents in the latter two alloys, which promote the precipitation of detrimental phases. EDS-analysis in the SEM supports this; emitted As-signals frequently overlapped with Al-signals in CW625N and CW626N, as illustrated in Figure 4, indicating that there are traces of the intermetallic particles arsenic particles in the form of aluminium arsenides, AlAs. These reportedly are related to dezincification and grain boundary attack [1, 5, 6, 10, 11]. Hence, it is possible that the higher aluminium content contributes to more frequent precipitation of intermetallic aluminium arsenide particles.
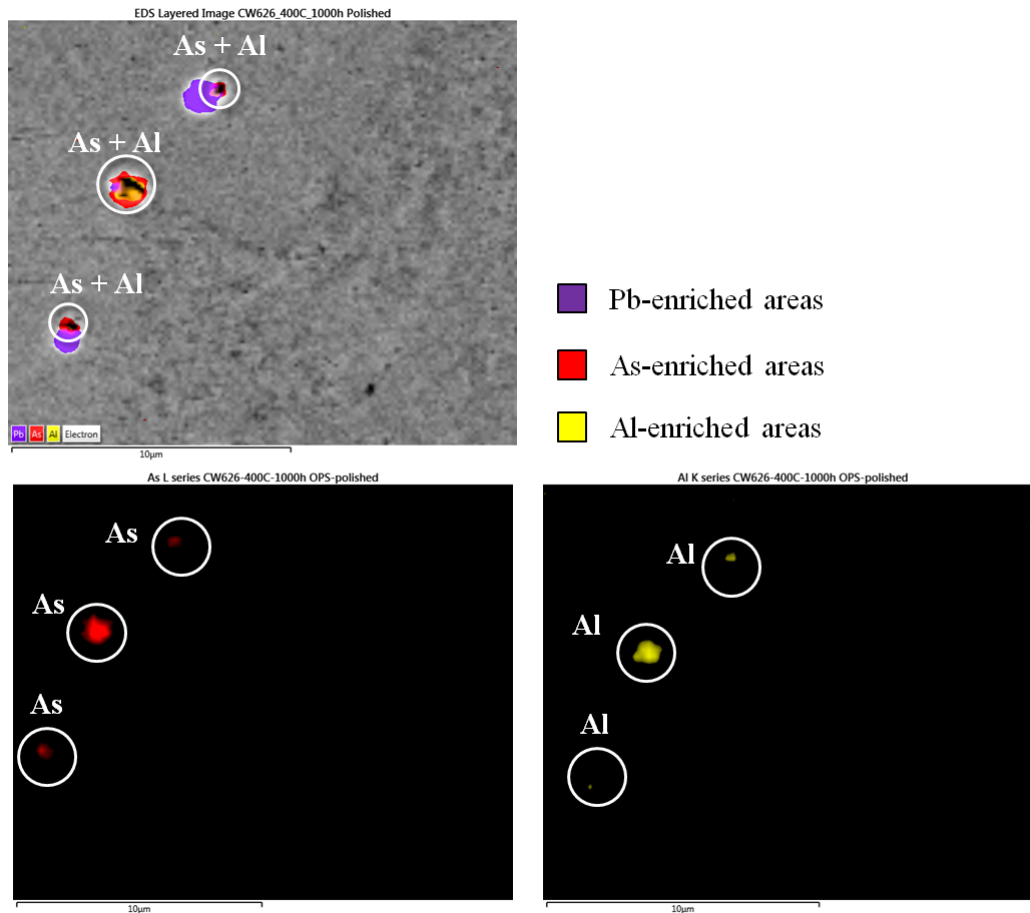
Figure 4: EDS-analysis of As-enriched areas in CW626N, annealed at 400°C for 1000h, overlapping with Al adjacent to Pb-particles.

Based on the work of Wessman et al. [6], Olivier et al. [2] and Claesson & Rod [9], it was expected that arsenic would form intermetallic particles with iron. However, as illustrated in Figure 5, in the EDS-analysis it was observed that emitted iron signals did not overlap with arsenic. Instead it overlapped in conjunction with other elements, such as chromium, silicon and phosphorus. This suggests that the iron did not formed particles with arsenic, and so did not contribute to the depletion of dezincification resistance to the same degree as aluminium. The reason for this could be that the iron content was too low to precipitate as iron arsenide particles and/or that aluminium has higher affinity for arsenic compared to iron.
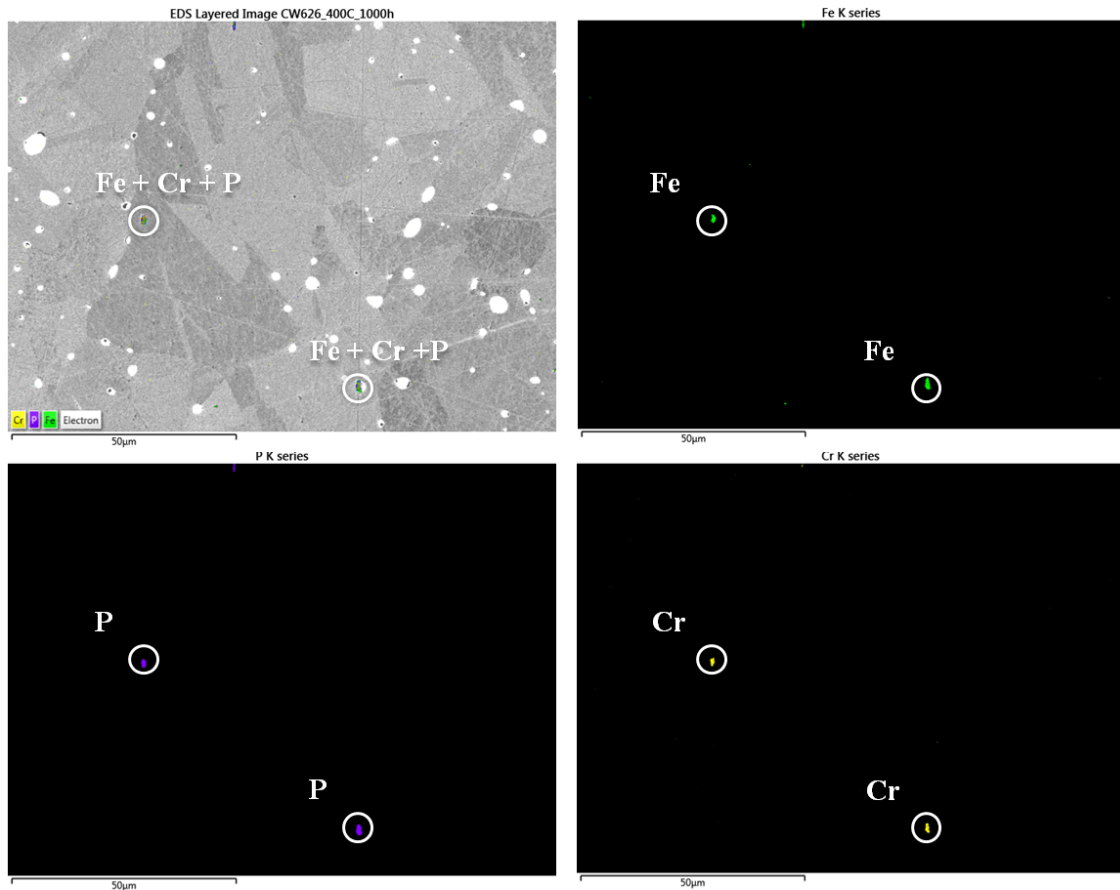
Figure 5: EDS-analysis of CW626N, displaying typical enriched areas of Fe overlapping with P and Cr at 2520x magnification.

By complementing the EDS signals with the EBSD image as displayed in Figure 6, it was observed that both the iron- and arsenic-enriched areas were visible along crystallographic defects, including grain boundaries, twins and adjacent to lead particles. This lends support to the aforementioned mechanism of dezincification by grain boundary attack [5, 11] since it indicates that the grain boundaries have lost dezincification resistance due to depletion of arsenic in solid solution with the α-phase. The results exemplified in Figure 6 also indicate that in addition to grain boundaries, the presence other defects such as twins or surfaces of undissolved particles (Pb in this instance) can provide nucleation sites for arsenic particles to form and thus result in loss of dezincification resistance.
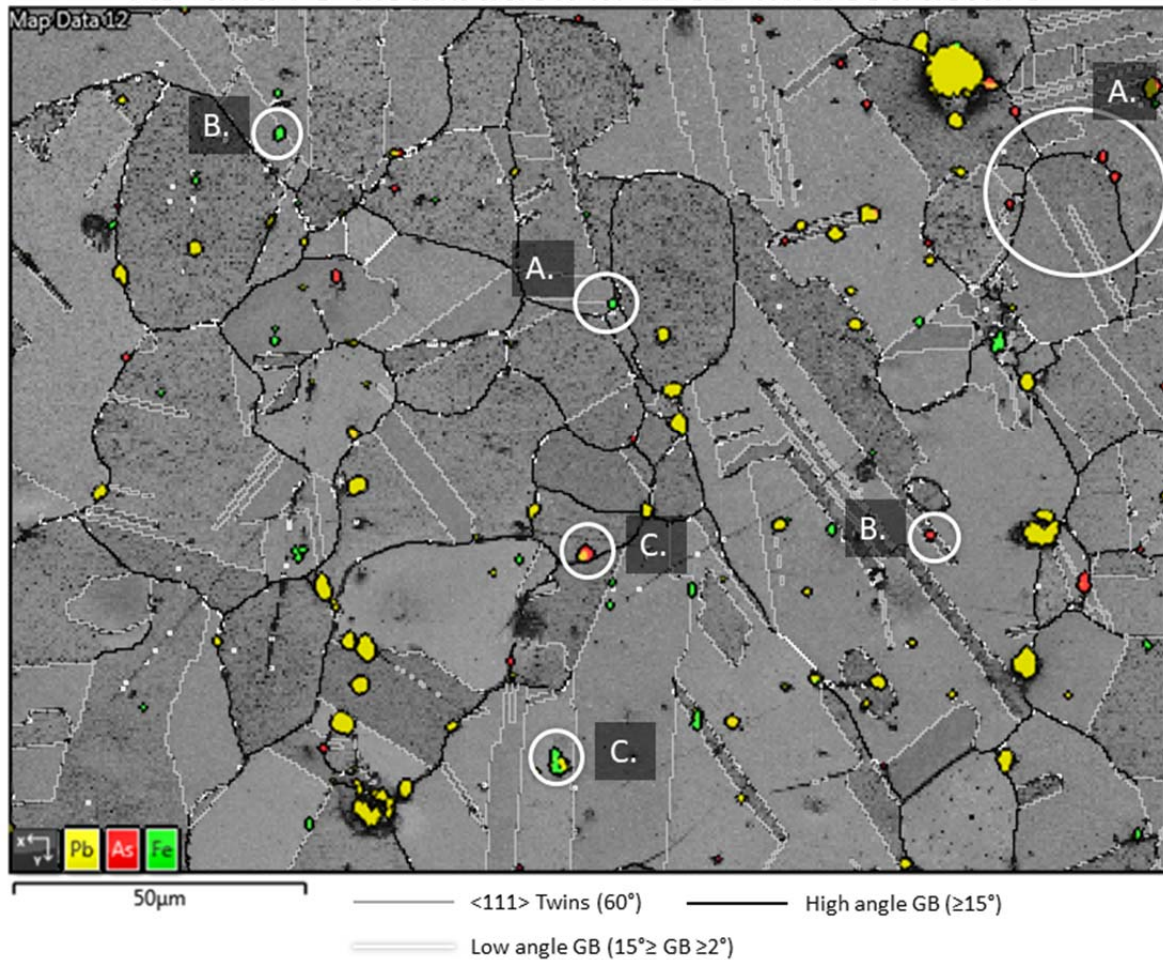
Figure 6: A composite image of sample CW626N-350°C-1000h, consisting of the result of EDS-analysis of As, Fe, and Pb as well as the EBSD-analysis of band contrast and grain boundaries. The highlighted areas exemplify how As and Fe overlap with: A) High angle grain boundaries, B) Twins (60°-boundaries) and C) Pb-particles.

With regard to β-phase, in CW625N and CW626N samples annealed at 250°C and 400°C, no traces of β-phase was observed in the etched microstructure using optical microscopy. It was only observable within samples annealed at 300°C, and to a lesser extent 350°C, for both CW625N and CW626N as illustrated in Figure 2 and 3. Since no β-phase was observed in the reference samples, it is plausible that this observed β-phase was caused as a result of the stress relieving heat treatment.

For CW625N- and CW626N-samples annealed at higher temperatures (350°C – 400°C), the area fraction of β-phase decreased, yet the corrosion resistance continued to decline while the relative frequency of As-particles increased. This strongly supports the view that it is

the formation of As-particles that is predominantly responsible for the decreased corrosion resistance at higher annealing temperatures.

At 300°C – 350°C, both β-phase and arsenic particles were observed in the microstructure of annealed samples and it is thus not clear the extent to which each phase contributes to the loss of dezincification resistance. However, since the CW625N annealed at 300°C for 1000h resulted in a large deterioration compared to the corresponding CW626N-sample, it is possible that the slightly larger area fraction of β-phase in CW625N contributed to the larger loss of dezincification resistance.
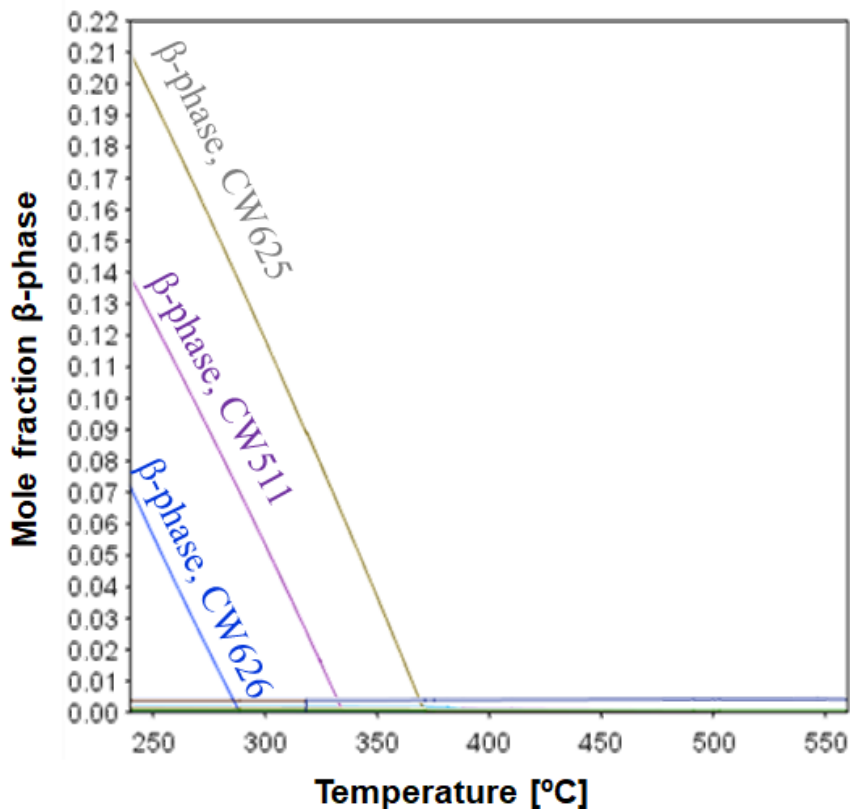

Figure 7: Thermodynamic calculations, displaying the mole fraction of precipitated β-phase in a homogenous steady state system as a function of temperature for the three alloys.

No β-phase was observed in CW511L. However, examination of the thermodynamic properties of β-phase in *Thermo-Calc* in Figure 7 implies that β-phase should be stable enough to precipitate in a homogenous steady state in this alloy system, even to a larger extent than in CW626N, which is not in agreement with the microstructural analysis. There is a possibility that the database for calculations is inadequate and gives an incorrect contribution from the aluminium component. In terms of the zinc content alone it would be expected that CW511L would be the most prone to form β-phase according to the simulated results. Alternatively, this

might be an effect of kinetics whereby aluminium accelerates the formation rate of β-phase due to differences in diffusivity.

In terms of what might cause CW625N to differ from CW626N, calculations in Figure 8 show that a higher copper/zinc-ratio coincides with a lower area fraction of β-phase. This provides a slight indication that the copper/zinc-ratio of the system can control the visible area fraction of β-phase, and thus the dezincification resistance. There is, however, a need to investigate the effect of this factor more systematically to properly evaluate its impact on the dezincification resistance.
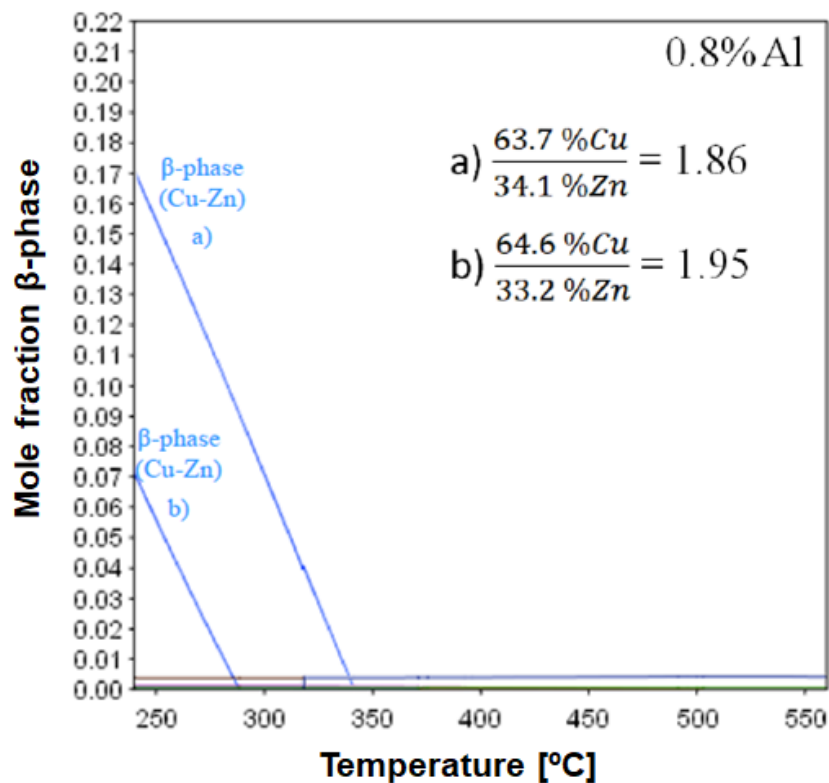

Figure 8: Two overlapping thermodynamic phase property diagrams with different Cu/Zn-ratio in order to illustrate how that factor impacts the stability of β-phase and thus controlling the mole fraction of β-phase able to precipitate.

The findings of this study will prove useful for the brass industry in the endeavour to adapt their processes to new low-lead and lead free brass components. The next step in completing the transition to lead free ecosystem is to demonstrate how the absence of lead in the new alloys affects the machinability of them. Additionally, one unresolved mechanistic aspect of this work is if the formation of intermetallic arsenic particles also depletes the arsenic atoms from the bulk of the grains in addition to the grain boundaries.

Conclusions

Brass alloys CW511L, CW625N and CW626N were stress-relief annealed from 2h to 1000h at temperatures in the range 250°C to 400°C in order to map how precipitated phases impact the dezincification behaviour.

Stress relieving heat treatments at temperatures higher than 250°C decrease the corrosion resistance only for the new low-lead alloys that contained aluminium, as a result of significant precipitation of β-phase and intermetallic aluminium arsenide particles. For the alloy without aluminium or iron, the corrosion resistance remained completely intact through the annealing process, regardless of temperature or annealing duration.

Intermetallic particles are formed adjacent to grain boundaries as well as on other crystallographic defects, including twins and undissolved lead particles. The thermodynamic simulations indicate that aluminium or iron may accelerate the formation of β-phase and that lower copper/zinc-ratio may be related to increased precipitation of β-phase.

Acknowledgements

References

[1]   Jacobsson D, Däcker CÅ, Sundberg R et al. A General Guide for Failure Analysis of Brass. Stockholm: Swerea KIMAB; 2005.

[2]   Oliver J, Hertzman S, Hutchinson B, et al. Dezincification of Brass - A Mechanistic Study. Stockholm: Swedish Institute of Metals research; 2000. (IM-2000; 045).

[3]   Davis DD. A note on the dezincification of brass and the inhibiting effect of elemental alloys. New York: Copper Development Association Inc; 1993.

[4]   Jones DA. Princliples and Prevention of Corrosion. New York (United States): Macmillan Publishing Company; 1992. Chapter 9.5, Princliples and Prevention of Corrosion; p. 322–332.

[5]   Sundberg R, Holm R, Hertzman S, et al. Dezincification (DA) and intergranular corrosion (IGA) of brass- Influence of composition and heat treatment. Stockholm: Swedish Institute of Metals research; 2003. (IM-2000; 045).

[6]   Wessman S, Oliver J, Nylén M, et al. Effect of stress relieving heat treatment on the corrosion of brass. Stockholm: Swerea KIMAB; 2007 (Swerea KIMAB Report 2007; 541)

[7]   Hutchinson B, Oliver J, Lindh-Ulmgren E, et al. Copper: Better properties for innovative products. Stockholm: Corrosion and Metals Research Institute (KIMAB); 2007. Chapter 19, Investigations into the Dezincification of α-Brass; p. 144–152.

[8]   Luo X, Yu J. The inhibition of the stress corrosion cracking of 70/30 brass in nitrite solution with additions of alloying arsenic and arsenic anions. Corros Sci. 1996; 38(5): 767–780.

[9]   Claesson E, Rod O. The effect of alloying elements on the corrosion resistance of brass. Mater Sci Technol. 2016; 32(17): 1794–1803.

[10]   Mazza F, Torchio S. Factors influencing the susceptibility to intergranular attack, stress corrosion cracking and de-alloying attack of aluminium brass. Corros Sci. 1983; 23(10): 1053-1072

[11]   Sundberg R, Hertzman S, Linder M. Copper: Better properties for innovative products. Stockholm: Corrosion and Metals Research Institute (KIMAB); 2007. Chapter 20, Intergranular Corrosion (IGA) of Brass; p. 153–163.

[12]   4MS Joint Management Committee. Acceptance of metallic materials used for products in contact with drinking water Part B – 4MS Common Composition List. Seville: 4MS Joint Management Committee; 2013.

[13]   nordicbrass.se [Internet]. Sweden: Nordic Brass Gusum AB; 2018; [cited 2018 Feb 19]. Available: http://www.nordicbrass.se/en/products/rod-cw625n

[14]   Swedish Standard Institute. Corrosion of metals and alloys – Determination of dezincification resistance of copper alloys with zinc – Part 1: Test method (ISO 6509-1:2014), Stockholm: Swedish Standard Institute; 2014. Standard SS-EN ISO 6509-1:2014.